ELSEVIER

Journal of Chromatography A, 893 (2000) 23–35

JOURNAL OF CHROMATOGRAPHY A

www.elsevier.com/locate/chroma

Preparation and evaluation of packed capillary columns for the separation of nucleic acids by ion-pair reversed-phase high-performance liquid chromatography

Herbert Oberacher[a], Alexander Krajete[a], Walther Parson[b], Christian G. Huber[a,*]

[a]*Institute of Analytical Chemistry and Radiochemistry, Leopold-Franzens University, Innrain 52a, A-6020 Innsbruck, Austria*
[b]*Institute of Legal Medicine, Leopold-Franzens University, Müllerstrasse 44, A-6020 Innsbruck, Austria*

Received 3 February 2000; received in revised form 29 June 2000; accepted 30 June 2000

Abstract

Oligonucleotides and double stranded DNA fragments were separated in 200 μm I.D. capillary columns packed with micropellicular, octadecylated, 2.1 μm poly(styrene–divinylbenzene) particles by ion-pair reversed-phase high-performance liquid chromatography (IP-RP-HPLC). Both the length and the diameter of the connecting capillaries (150×0.020 mm I.D.) as well as the detection volume (3 nl) had to be kept to a minimum in order to maintain the high efficiency of this chromatographic separation system with peak widths at half height in the range of a few seconds. Three different types of frits, namely sintered silica particles, sintered octadecylsilica particles, and monolithic poly(styrene–divinylbenzene) (PS–DVB) frits were evaluated with respect to their influence on chromatographic performance. Best performance for the separation of oligonucleotides and long DNA fragments was observed with the PS–DVB frits, whereas the short DNA fragments were optimally resolved in columns terminated by octadecylsilica frits. The maximum loading capacity of 60×0.20 mm I.D. columns ranged from 20 fmol (7.7 ng) for a 587 base pair DNA fragment to 500 fmol (2.4 ng) for a 16-mer oligonucleotide. Lower mass- and concentration detection limits in the low femtomol and low nanomol per liter range, respectively, make capillary IP-RP-HPLC with UV absorbance detection highly attractive for the separation and characterization of minute amounts of synthetic oligonucleotides, DNA restriction fragments, and short tandem repeat sequences amplified by polymerase chain reaction.

Keywords: Ion-pair chromatography; Capillary columns; poly(styrene–divinylbenzene) stationary phases; Stationary phases, LC; Short tandem repeats sequences; Forensic analysis; Oligonucleotides; DNA

1. Introduction

One of the clear trends in modern science and technology is miniaturization [1]. This trend is also a permanent goal of analytical chemistry where the growing interest in analyzing minute samples of high complexity is the driving force for the rapid development of miniaturized techniques [2]. Consequently, the modern practice of analyzing complex mixtures of biological origin has profoundly benefited from the miniaturization of chromatographic separation techniques [3,4]. Basically, four major advantages connected with the use of columns in the capillary format (10–500 μm I.D.) for high-performance

*Corresponding author. Tel.: +43-512-507-5176; fax: +43-512-507-2767.

E-mail address: christian.huber@uibk.ac.at (C.G. Huber).

0021-9673/00/$ – see front matter
PII: S0021-9673(00)00731-7

liquid chromatography (HPLC) can be specified: (1) better resolving power can be accomplished in shorter time [5,6]; (2) the reduced sample requirement of miniaturized HPLC eliminates the need to prepare large amounts of sample [4]; (3) on-line conjugation to mass spectrometry is feasible [7,8]; and (4) expenses connected with consumption and disposal of chemicals and materials are cut down. The improved separation efficiency of capillary columns is attributed to decreased flow dispersion and a very homogenous packing bed structure, in which the stabilizing influence of the wall is exhibited across the entire packing bed [6]. As the volume of eluent pumped through a capillary column is reduced, the solutes of interest are dissolved in much less eluent, resulting in higher mass sensitivity and easier coupling with mass spectrometry.

Despite considerable advances in packing technology, the present day status of manufacturing capillary columns is still more of an art [9–11]. Because of the small column volume, any local irregularities of the packing can produce a dramatic reduction in column efficiency. Nevertheless, Hsieh and Jorgenson demonstrated reduced plate heights as small as 1.0–1.2 with 12 μm I.D. capillary columns packed with 5 μm YMC ODS-AQ C_{18} silica particles [12]. Presently, stationary phases based on porous silica gel are most frequently used for packing microcolumns although, in conventional HPLC, micropellicular, polymeric packing materials have been shown to provide excellent chromatographic properties for biopolymer separations [13–15]. An important part of capillary column technology is the placement of a small frit that retains the packing material inside the capillary [16]. The correct choice of the frit material is important because adsorption of analytes that elute from the column causes decreased sample recovery and loss of column performance. Various techniques have been developed to hold the particles in the column such as the use of a piece of quartz wool [17], a small, porous PTFE disk [16], a special ceramic frit support [18], and sintered glass beads [19]. With siliceous stationary phases, the frits can be made directly from the packing material by sintering a tiny segment of silica particles with the help of an electrically heated filament ring [20]. Subsequent deactivation of the silica frits by silanization has been shown to considerably reduce adsorption and peak broadening [21].

Capillary HPLC instrumentation must be configured with low injection volumes, be able to deliver reproducible gradients at low flow-rates, and requires a sensitive detector with a low volume detection cell [22]. The small peak volumes and the high efficiency that can be attained with micropellicular packing materials require that all contributions to extra column volume are kept to an absolute minimum. Moreover, to avoid peak dispersion during detection, the detection volume should not be more than one tenth of the volume of the peak that is leaving the separation column. One disadvantage of micropellicular stationary phases compared to porous stationary phases is the decrease in surface area and, hence, sample loading capacity [23]. Therefore, the dynamic range of UV detection is restricted because the injection of relatively large solute concentrations results in peak dispersion due to column overloading.

While application of HPLC columns of conventional dimensions has been very useful for the analysis of nucleic acids [15,24], there are only few reports on the utilization of capillary HPLC for nucleic acid separations [25,26]. Recently, we reported on the application of 200 μm I.D. capillary columns for the separation of oligonucleotides up to 40 nucleotides by ion-pair-reversed-phase HPLC (IP-RP-HPLC) [27]. In this study we investigated the applicability of such capillary columns to the separation of oligonucleotides longer than 40 nucleotides and of double stranded DNA fragments ranging in size from 51 to 2176 base pairs (bp). The influence of frit material and sample loading on column performance as well as selected examples of application are discussed.

2. Experimental

2.1. Chemicals and nucleic acid samples

Acetonitrile (HPLC gradient-grade), methanol (HPLC gradient-grade), tetrahydrofuran (analytical reagent grade), styrene (synthesis grade), and divinylbenzene (synthesis grade) were obtained from Merck (Darmstadt, Germany). Styrene and divinylbenzene were distilled before use. Decanol (synthesis grade) and azobisisobutyronitrile (synthesis grade) were from Fluka (Buchs, Switzerland). A 1.0 *M* stock solution of triethylammonium acetate

(TEAA) was prepared by dissolving equimolar amounts of triethylamine (analytical reagent grade, Fluka) and acetic acid (analytical reagent grade, Fluka) in water. A 1.0 *M* stock solution of triethylammonium bicarbonate (TEAB), pH 8.4–8.8, was prepared by passing carbon dioxide gas (AGA, Vienna, Austria) into a 1.0 *M* aqueous solution of triethylamine at 5°C until the desired pH was reached. For preparation of all aqueous solutions, high-purity water (Epure, Barnstead, Newton, MA, USA) was used. The pH of the eluents was adjusted with an accuracy of ±0.05 units and the given pH values always correspond to the neat aqueous solutions before addition of organic solvent. The standards of phosphorylated and non-phosphorylated oligonucleotides [$(dT)_{12-18}$, $p(dA)_{12-18}$, $p(dA)_{40-60}$, $(dT)_{16}$] were purchased as sodium salts from Pharmacia (Uppsala, Sweden) or Sigma–Aldrich (St. Louis, MO, USA). Size standards of double-stranded DNA restriction fragments were purchased from Boehringer Mannheim (mixture of a pBR328 DNA-*Bgl* I and a pBR328 DNA-*Hin*f I digest, Mannheim, Germany), USB (pBR322 DNA-*Msp* I digest, United States Biochemical, Cleveland, OH, USA), and Sigma Aldrich (pBR322 DNA-*Hae* III digest and pUC18 DNA-*Hae* III digest). The separated DNA fragments are identified in chromatograms and tables by their respective length in bp (1 bp=660 Da). The synthetic 80-mer oligonucleotide was obtained from Microsynth (Balgach, Switzerland) and used without further purification. Its sequence was the same as the reverse complementary sequence in the pBR322 plasmid from position 3410–3489 relative to the *Eco*R I recognition site.

2.2. Preparation of frits and packing of capillary columns

Polyimide coated fused-silica capillary tubing of 350 μm O.D. and 200 μm I.D. was obtained from Polymicro Technologies (Phoenix, AZ, USA). A retaining frit was made at the end of a 15 cm long fused-silica capillary by sintering a thin slug of 2.0 μm nonporous silica particles (Glycotech, Hamden, CT, USA) wetted with a small droplet of sodium silicate solution (Sigma–Aldrich) by means of an electrically heated nickel–chrome filament ring. A slurry reservoir of 50 mm length, 6.35 mm O.D., 2.45 mm I.D. and having an internal volume of 236 μl was fabricated from stainless steel tubing (Alltech, Deerfield, IL, USA) and a pair of column end fittings (Valco, Houston, TX, USA), with the holes of the fittings drilled to a diameter of 0.50 mm. The open end of the capillary was connected to the slurry reservoir with approximately 2 mm of the capillary protruding into the reservoir. Octadecylated poly(styrene–divinylbenzene) particles (PS–DVB–C_{18}, 2.3 μm) were prepared according to the previously published protocol [28]. Five milligrams of the PS–DVB–C_{18} stationary phase were suspended in 260 μl tetrahydrofuran, sonicated for 10 min, and transferred to the slurry reservoir. The column was packed with methanol at a constant pressure of 70 MPa using an air-driven packing pump (Knauer, Berlin, Germany) until the length of the packed section in the column was 70–90 mm which took approximately 25 min. Then, the flow of the packing solvent was stopped and after slowly releasing the pressure, the column was flushed with bidistilled water at 70 MPa for 90 min before it was removed from the slurry reservoir and trimmed to a length of 60 mm. No frit was made at the inlet end of the capillary column.

Frits consisting of octadecylated silica particles were prepared by packing 2.0 μm nonporous octadecyl silica particles (Glycotech) into a 200 μm I.D. fused-silica capillary having a silica retaining frit at the end. A small section of the octadecyl silica particles was sintered with an electrically heated nickel–chrome filament ring while flushing the capillary with water. The retaining frit was cut off and the excess of non sintered material was washed out. The procedure for preparation of monolithic poly(styrene–divinylbenzene) (PS–DVB) frits was as follows. First, a 1 m piece of 200 μm I.D. fused-silica capillary tubing was silanized with 3-(trimethoxysilyl)propyl methacrylate according to the procedure published in Ref. [29] in order to ensure immobilization of the frit at the capillary wall. Then, the first 50 mm of a 200 mm piece of the silanized capillary were filled with a mixture comprising 50 μl styrene, 50 μl divinylbenzene, 150 μl decanol, and 2.5 mg azobisisobutyronitrile by capillary action. The mixture was polymerized at 80°C for 24 h. After polymerization, the polymer frit was cut to a length of 0.5 mm and extensively flushed with tetrahydrofuran at a flow-rate of 10 μl/min. Columns terminated with octadecyl silica or polymeric frits were

packed with PS–DVB–C_{18} particles using the same procedure as described above.

2.3. High-performance liquid chromatography

The HPLC system consisted of a low-pressure gradient micro pump (model Rheos 4000, Flux Instruments, Karlskoga, Sweden) controlled by a personal computer, a vacuum degasser (Knauer, Germany), a column thermostat made from 3.3 mm O.D. copper tubing which was heated by means of a circulating water bath (model K 20 KP, Lauda, Lauda-Königshofen, Germany), a microinjector (model C4-1004, Valco) with a 20 nl or 500 nl internal sample loop, a variable wavelength detector, and a personal computer (PC)-based data system (Chromeleon 4.30, Dionex-Softron, Germering, Germany). The UV detectors were from Linear Instruments (model Linear UV–VIS 200, Linear Instruments, Fremont, CA, USA) and LC Packings (model UltiMate UV detector, LC Packings, Amsterdam, Netherlands). The detection cells combined with the detectors were a laboratory prepared capillary bubble cell prepared by etching of a 375 μm O.D.×20 μm I.D. fused-silica capillary, a Z-shaped UZ-LI-NAN, 3 nl cell (LC Packings [30]), a UZ-ULT-N10, 3 nl cell (LC Packings), or a UZ-ULT-C10, 45 nl cell (LC Packings). The inner diameters of the capillaries used in the commercial detection cells were 20 μm for the 3 nl cells and 75 μm for the 45 nl cell, respectively. The four different UV detector/detection cell combinations used in this study are summarized in Table 1. A primary flow of 100–120 μl/min was split by a ratio of 1:30–1:60 to 2.0–3.5 μl/min with the help of a T-piece and a 50 μm I.D. fused-silica restriction capillary. The injection volume was 500 nl for all separations except for the chromatogram shown in Fig. 6, where it was 20 nl. The column temperature was set to 50°C and the column effluent was monitored at 254 nm.

For micropreparative isolation of DNA fragments a 60×4.0 mm I.D. column packed with PS–DVB–C_{18} and an HPLC system comprising a low pressure gradient pump (Model 480 GT, Gynkotek, Germering, Germany), a degasser (Knauer, Germany), a column oven (Model STH 585, Gynkotek), a diode array UV detector (Model UVD-320, Gynkotek) set at 254 nm, a sample injection valve (Model 9125, Rheodyne, Cotati, CA, USA) with a 20 μl sample loop, and a PC-based data system (GynkoSoft, Version 5.50, Gynkotek) were used. Approximately 2–3 μg of a pUC18-DNA *Hae* III restriction digest in 10 μl were loaded onto the column for micropreparative separation of DNA fragments and separated with a gradient of 8.75–13.25% acetonitrile in 3.0 min, followed by 13.25–15.0% acetonitrile in 7.0 min in 100 m*M* TEAA at a flow-rate of 750 μl/min. The isolated 174 bp, 298 bp, and 587 bp fragments were lyophilized to dryness and the residue was redissolved in water. The DNA concentration in the fractions was determined by comparison of the peak areas of the fractions with those of a standard of known concentration.

2.4. Polymerase chain reaction (PCR)

PCR was performed in 0.5 ml MicroAmp reaction tubes (Perkin-Elmer, Foster City, CA, USA) by adding 2 ng of DNA to a total volume of 50 μl of PCR Buffer II (Perkin-Elmer), 1.5 m*M* $MgCl_2$, 0.2 m*M* of each dNTP, 0.5 μ*M* of each primer (humTH01f 5′-CCTGTTCCTCCCTTATTTCCC; humTH01r 5′-GGGAACACAGACTCCATGGTG, biotinylated) and 1.25 U TaqGold DNA Polymerase (Perkin-Elmer). Amplification was carried out in a 9600 GeneAmp thermocycler (Perkin-Elmer) comprising 32 cycles of 94°C denaturation for 30 s, 58°C

Table 1
Detector/detection cell combinations used in this study

No.	Detector	Detection cell	Diameter of the connecting capillary[a]
1	UltiMate	UZ-ULT-C10, 45 nl	75 μm
2	UV–VIS 200	UZ-LI-NAN, 3 nl	20 μm
3	UV–VIS 200	capillary bubble cell	20 μm
4	UltiMate	UZ-ULT-N10, 3 nl	20 μm

[a] Length of the capillary connection from column outlet to detection cell: 150–200 mm.

annealing for 15 s, and 72°C extension for 30 s. Prior to amplification the enzyme was activated by a 95°C incubation for 11 min. Finally, samples were cooled to room temperature.

3. Results and discussion

3.1. Influence of detector and detector cell on chromatographic performance

Using UV absorption to detect the analytes separated by capillary HPLC, the sensitivity is proportional to the path length of the flowcell according to Lambert–Beer's law. Additionally, to minimize short-term noise, the flowcell aperture should be relatively large. This requires a relatively large volume for sensitive detection. However, in order to avoid notable peak dispersion and to maintain the performance of the capillary HPLC system, all volumes, including injection-, detection-, and connecting volumes, must be downscaled by a factor $f = d^2_{conventional} / d^2_{capillary}$, where $d_{conventional}$ and $d_{capillary}$ are the diameters of the conventional and the capillary columns, respectively [22]. Consequently, a compromise between maximum sensitivity and minimum peak dispersion must be found. Downscaling from a 4.6 mm I.D. column to a 200 μm I.D. capillary column equals a factor 529. Applied to a detection volume of 10 μl for conventional HPLC, a volume of approximately 20 nl should be appropriate for capillary HPLC.

Fig. 1 illustrates the influence of four different detector configurations on detection performance with oligonucleotides. A standard of oligodeoxythymidylic acids was separated in a 200 μm I.D. capillary column packed with micropellicular PS–DVB–C_{18} particles. With a 45 nl Z-shaped capillary flowcell mounted on the UltiMate detector, the seven oligonucleotides were detected as almost ideal gaussian peaks with a signal-to-noise ratio of 116:1 and an average peak width at half height of 7.7 s (Fig. 1a). The peak widths were significantly reduced using a 3 nl Z-shaped capillary flowcell combined with the Linear detector at the cost of a dramatic loss in signal-to-noise ratio (1.6:1, Fig. 1b). However, an improvement of the signal-to-noise ratio to 5.2:1 was achieved with the Linear detector by using a capillary bubble cell (Fig. 1c). The reduction in average peak width at half height from 7.7 to 4.3 s indicated considerable peak dispersion with the 45 nl flowcell, which is made from 75 μm I.D. fused-silica tubing. The detection volume of the capillary bubble cell is difficult to calculate since the width of the light beam passing through the capillary is not exactly known. Assuming a width of 0.5 mm for the light beam and an inner capillary diameter of 275 μm, the bubble cell had a volume of approximately 30 nl. Consequently, the improved efficiency observed with the capillary bubble cell is attributable both to reduced peak dispersion in the 20 μm I.D. capillary connect-

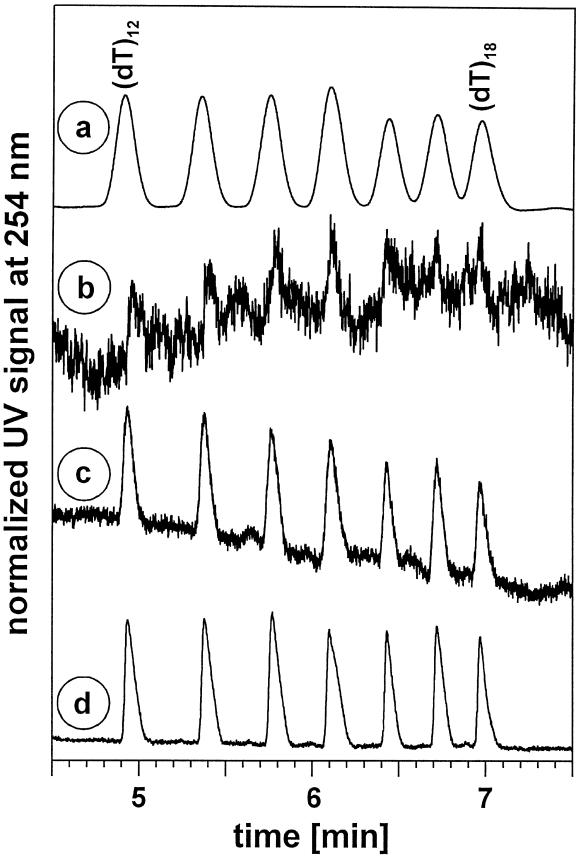

Fig. 1. Influence of detector and detection cell on detectability and chromatographic performance. Column, PS–DVB–C_{18}, 2.1 μm, 60×0.20 mm I.D. with silica frit; mobile phase, (A) 100 m*M* TEAA, pH 7.0, (B) 100 m*M* TEAA, pH 7.0, 20% acetonitrile; linear gradient, 25–60% B in 10.0 min; flow-rate, 2.6 μl/min; sample, $(dT)_{12-18}$, 0.71 ng each; detector/detection cell combinations (see Table 1), (a) No. 1, (b) No. 2, (c) No. 3, (d) No. 4.

ing the column and the detector cell and a lower detection volume. The best detection performance in terms of detectability and low peak dispersion was obtained with the UltiMate detector in combination with a 3 nl Z-shaped capillary flowcell, which resulted in a signal-to-noise ratio of 20.6:1 and an average peak width at half height of 3.5 s (Fig. 1d). The reduction in peak width at half height with the different configurations was accompanied by an increase in peak asymmetry (average asymmetry factors of 1.12, 1.67, and 2.11 in Fig. 1a, c, and d, respectively). There are two possible explanations for the observed increase in peak asymmetry with the more efficient detector cells. First, the asymmetry could be inherent to the chromatographic separation process but is only detectable with the high efficiency detector cells, whereas less efficient cell configurations tend to hide the peak asymmetry. Second, asymmetry could be introduced after separation by some unknown peculiarity of the detector cell construction, which is most pronounced with the low-volume detection cells. For further experiments, either the combination Linear detector-capillary bubble cell or the combination UltiMate detector-Z-shaped 3 nl capillary flowcell were used.

3.2. Influence of different frit materials on chromatographic performance

Although several procedures for the preparation of frits for capillary columns are described in the literature [10], only few investigators have reported on the influence of different frit designs and materials on chromatographic performance [21,31,32]. Our motivation to use different frit materials stems from the finding, that oligonucleotides and DNA fragments can be separated with high efficiency by IP-RP-HPLC on micropellicular, octadecyl–PS–DVB beads, but not on micropellicular octadecylsilica beads [28,33]. The poor chromatographic performance of silica-based stationary phases was attributed to silanol interactions, which are expected to be also effective with silica-based frits. However, since the frit contributes to only about 1% of the total column length, the effect of the small frit on chromatographic performance has to be elucidated.

For the evaluation of different frit materials, a $(dT)_{12-18}$ oligonucleotide standard and a pBR322 DNA-*Hae* III digest were separated in 60×0.2 mm capillary columns terminated by three different frits, namely silica-, octadecylsilica-, and monolithic PS–DVB frits. Table 2 summarizes the resolution values for two selected pairs of oligothymidylic acids. It can be seen that the resolution of oligonucleotides increased with the different frits in the order silica< octadecylsilica<PS–DVB frits. Taking the resolution of the PS-DVB frits as 100%, the performance of the silica and octadecylsilica frits was 89% and 95%, respectively for the pair $(dT)_{12}/(dT)_{13}$, and 90% and 91%, respectively, for the pair $(dT)_{17}/(dT)_{18}$. This trend confirms the assumption that oligonucleotides interact with the silanol groups of the frit materials and that these interactions are attenuated by chemical deactivation of the silica with octadecyl groups or eliminated by the use of a polymeric frit material. The high efficiency with the polymeric frits can be attributed to their high permeability, allowing faster and more efficient packing of the columns, and the chemical similarity between the stationary phase and the frit material, PS–DVB-based polymer in both cases.

The scanning electron micrographs of the three types of frits depicted in Fig. 2 revealed some significant differences in the morphology of the frits. The frits prepared from silica particles were relatively inhomogeneous and some of the channels between the particles were blocked with silica gel because sodium silicate solution was added to glue

Table 2
Resolution R of selected pairs of oligonucleotides in capillary columns with different frits

Frit type	R [a] $(dT)_{12}/(dT)_{13} \pm s_d/N^{1/2}$	R [a] $(dT)_{17}/(dT)_{18} \pm s_d/N^{1/2}$
Silica	3.444±0.049	2.167±0.037
Octadecylsilica	3.610±0.082	2.188±0.039
PS–DVB	3.872±0.076	2.423±0.054

[a] The given values represent the average and standard deviation of the average $s_d/N^{1/2}$ of $N=30$ measurements on 5 different columns. Chromatographic conditions, flow-rate, 3.5 μl/min; detector/detection cell No. 3, other conditions as in Fig. 1.

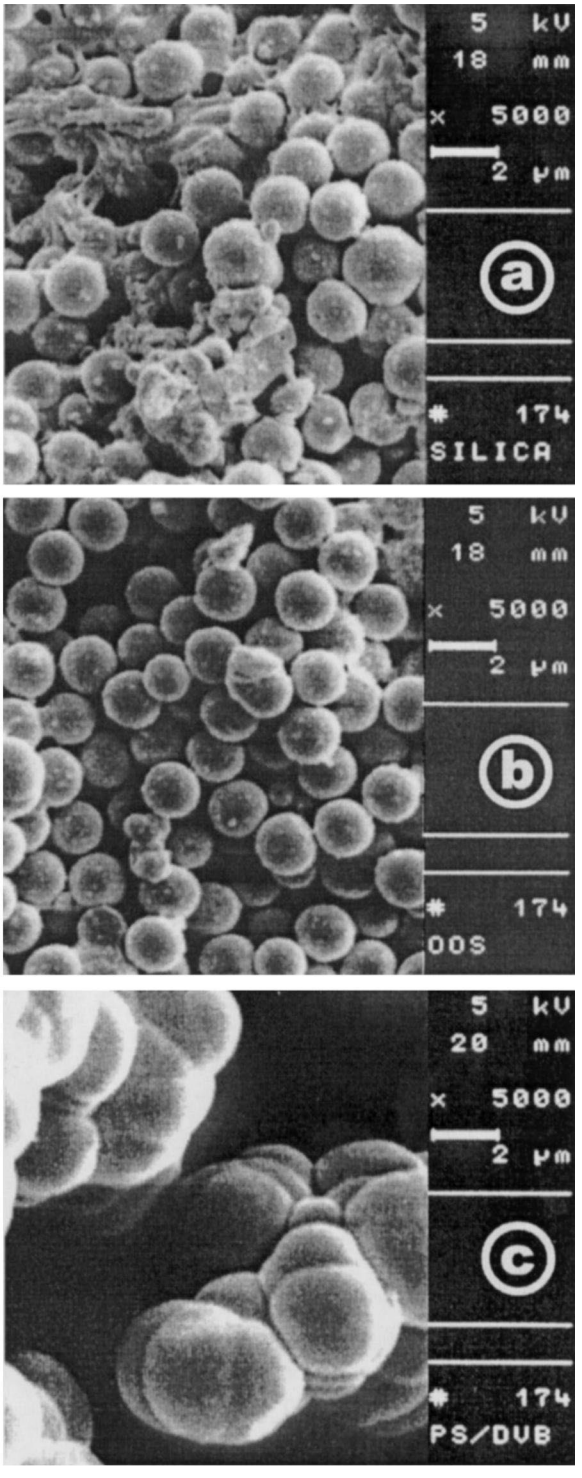

Fig. 2. Scanning electron micrographs showing the morphology of (a) sintered silica, (b) sintered octadecylsilica, and (c) monolithic PS–DVB frits at 5000-fold magnification.

the particles together (Fig. 2a). Sintering of packed octadecylsilica particles yielded a more uniform frit structure with all intraparticular channels left open (Fig. 2b). Very large channels are formed in the monolithic structure due to the phase separation, which occurs during the polymerization of styrene and divinylbenzene in the presence of decanol as porogen (Fig. 2c). These large channels make the monolithic frits highly permeable, while the rigid porous polymer, which is covalently attached to the column wall, offers sufficient mechanical stability to allow column packing at pressures up to 100 MPa. The standard deviations of the resolution values give some insight in the reproducibility of the preparation of capillary columns, including frit preparation and column packing. The relative standard deviations for the resolution of $(dT)_{12}$ and $(dT)_{13}$ on five columns each, terminated by silica-, octadecylsilica-, and PS–DVB frits, were 7.9%, 12.4%, and 10.7%, respectively, which are good values for the preparation of capillary columns.

The improved performance of PS–DVB–C_{18} columns with PS–DVB frits allowed the high-resolution separation of homooligonucleotides up to a chain length of 60 nucleotides by capillary IP-RP-HPLC, which was previously not possible on columns terminated by silica frits. Fig. 3 depicts the separation of phosphorylated oligodeoxyadenylic acids containing 12–60 adenine units. Applying a gradient of 4.5–7.0% acetonitrile in 5 min, followed by 7.0–8.5% acetonitrile in 10 min in 100 m*M* triethylammonium acetate, oligonucleotides up to the 50-mer were separated to baseline with peak widths at half height ranging from 2.5 to 9.4 s. Thereafter, resolution slowly decreased with longer oligonucleotides.

With double-stranded (ds) DNA fragments, the chromatographic efficiency observed with the different frit designs depended on the size of the DNA fragments. For fragments shorter than approximately 250 bp, octadecylsilica frits yielded the best results, whereas maximum resolution for longer fragments was obtained with PS–DVB frits (Table 3). Taking the resolution with the octadecyl frits as 100%, the resolution values with silica frits ranged from 74 to 88%, those with the PS–DVB frits from 86 to 110%. The better performance of PS–DVB frits for long DNA fragments might be attributed to a more open porous structure of the channels in the polymeric

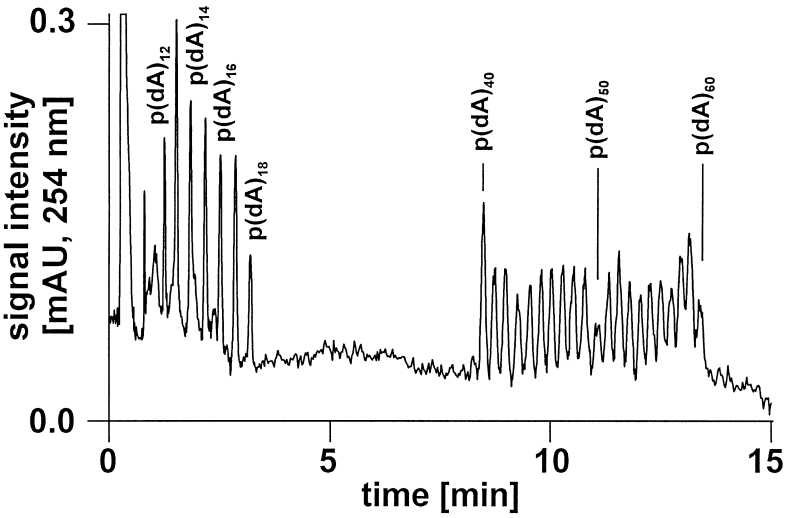

Fig. 3. Separation of oligonucleotides ranging in size from 12 to 60 nucleotides. Column, PS–DVB–C_{18}, 2.1 μm, 60×0.20 mm I.D. with PS–DVB frit; mobile phase, (A) 100 m*M* TEAA, pH 7.0, (B) 100 m*M* TEAA, pH 7.0, 25% acetonitrile; linear gradient, 18–28% B in 5.0 min, 28–34% B in 10.0 min; flow-rate, 2.0 μl/min; detector/detection cell No. 4; sample, $p(dA)_{12-18}$, 0.36 ng each, $p(dA)_{40-60}$, 0.24 ng each.

frits compared to the rather small diameter channels in the silica-based frits, which may cause restricted diffusion in the channels (Fig. 2).

3.3. Analytical loading capacity of capillary columns for oligonucleotides and dsDNA fragments

Due to the non-linearity of adsorption isotherms in liquid chromatography, peak shapes are distorted and broadened at high sample loads. Therefore, for optimum analytical performance the maximum amount of sample loaded onto a column is usually chosen such that the loss in separation efficiency does not exceed 10%. The loading capacity of a 60×0.2 mm I.D. capillary column for oligonucleotides and DNA fragments was evaluated by injecting increasing amounts of $(dT)_{16}$ and 174 bp, 298 bp, and 587 bp DNA fragments, that have been isolated from a pUC18-DNA *Hae* III digest by micropreparative IP-RP-HPLC. Subsequently, the peak widths at half height were plotted against the sample load (Fig. 4). The maximum analytical loading capacities for a 60×0.2 mm I.D. column that were deduced from the graphs were 2.4 ng (500 fmol) for $(dT)_{16}$, 11 ng (100 fmol) for 174 bp DNA, 16 ng (80 fmol) for 298 bp DNA, and 7.7 ng (20 fmol) for 587 bp DNA. It can be seen, that the mass loading capacity was in the same order of magnitude both for oligonucleotides and DNA fragments (2.4–16 ng). However, the loading capacity in terms of amount of substance decreases with increasing molecular mass of the

Table 3
Resolution R of selected pairs of DNA fragments in capillary columns with different frits

Frit type	R [a] 57/64±$s_d/N^{1/2}$	R [a] 89/104±$s_d/N^{1/2}$	R [a] 213/234±$s_d/N^{1/2}$	R [a] 434/458±$s_d/N^{1/2}$
Silica	3.12±0.20	3.97±0.20	2.70±0.13	1.09±0.086
Octadecylsilica	3.67±0.12	5.38±0.18	3.29±0.12	1.24±0.056
PS–DVB	3.52±0.083	4.64±0.12	3.17±0.18	1.37±0.064

[a] The given values represent the average and standard deviation of the average $s_d/N^{1/2}$ of $N=30$ measurements on 5 different columns. Chromatographic conditions, linear gradient, 35–67% B in 3.0 min, 67–82% B in 12.0 min; flow-rate, 2.5 μl/min; detector/detection cell, No. 4; sample, 4.6 ng pBR322 DNA-*Hae* III digest.; other conditions as in Fig. 1.

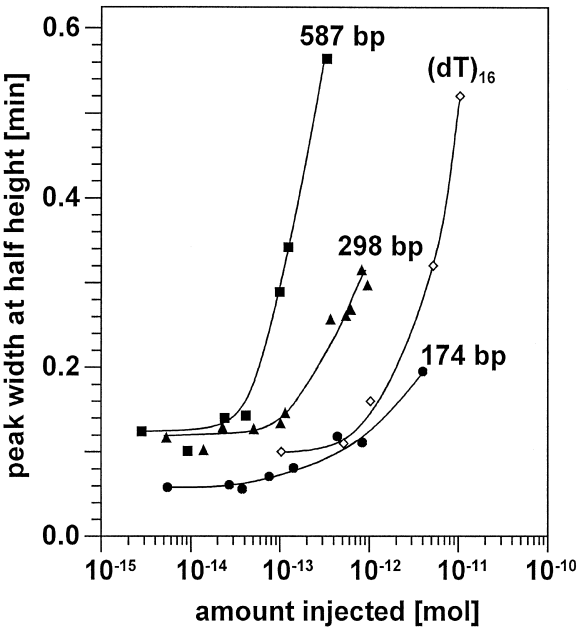

Fig. 4. Loading capacity of a 60×0.20 mm capillary column for oligonucleotides and dsDNA fragments of different size. Column, PS–DVB–C_{18}, 2.1 μm, 60×0.20 mm I.D. with silica frit; mobile phase, (A) 50 m*M* TEAB, pH 8.4, (B) 50 m*M* TEAB, pH 8.4, 20% acetonitrile; linear gradient, 25–60% B in 10.0 min for $(dT)_{16}$; 35–53% B in 3.0 min, 53–65% B in 7.0 min for the DNA fragments; flow-rate, 2.9 μl/min for $(dT)_{16}$, 2.4 μl/min for the DNA fragments; detector/detection cell No. 4; sample, $(dT)_{16}$, 174 bp, 298 bp, and 587 bp fragments of the pUC18 DNA-*Hae* III digest.

nucleic acids (500–20 fmol) as a consequence of increasing molecular size of the analytes. Moreover, among the DNA fragments the curvature of the plots of peak width at half height *versus* injected amount increases with the size of the DNA fragments, which means that peak broadening due to overloading becomes more severe with larger DNA fragments. This is especially important for the separation of fragments in DNA restriction digests, where all fragments are present in equimolar amounts.

Fig. 5 illustrates the effect of overloading on chromatographic performance by the separation of a pBR322 DNA-*Hae* III digest. Injection of 490 ng digest, corresponding to an amount of 182 fmol for each DNA fragment, resulted in relatively sharp and symmetric peaks for fragments smaller than 150 bp, whereas peak broadening and tailing due to overloading were evident with DNA fragments larger than 150 bp (Fig. 5a). The peak widths at half height for the 104 bp and 267 bp fragments, for example, were 4.9 and 18.2 s, respectively. Separation of a sample solution that was diluted by a factor of 10 improved the chromatographic performance mainly for the large DNA fragments (Fig. 5b). The peak widths at half height for the 104 bp and 267 bp DNA fragments in Fig. 5b were 3.3 and 11.3 s, respectively, which represents a 5.5 and 38% reduction in peak widths compared to Fig. 5a. However, insufficient separation of the 434–587 bp fragments still indicated overloading. With 49 ng of sample the limit of detection of the linear detector/bubble cell combination was almost reached so that further dilution of the sample was possible only with a more efficient detection system. Fig. 5c shows the chromatographic analysis of 4.6 ng (1.7 fmol for each DNA fragment) pBR322 DNA-*Hae* III digest using the UltiMate detector with the 3 nl detection cell. The high efficiency of this system is reflected in peak widths at half height ranging from 1.4 s for the 104 bp fragment to 5.7 s for the 267 bp fragments and finally 14.8 s for the 587 bp fragment, which allowed the baseline separation even of the large fragments of this digest. Moreover, this separation proves that the separation of double stranded DNA fragments is possible in 200 μm I.D. capillary columns with a separation efficiency equivalent to that obtained with conventional 4.6 mm I.D. columns (compare, e.g., Fig. 1 in Ref. [33]).

3.4. Application of capillary IP-RP-HPLC to the analysis of synthetic oligonucleotides

Since the introduction of phosphoramidite chemistry, synthetic oligonucleotides can be prepared rather easily by automated solid-phase synthesis [34]. While short oligonucleotides containing up to 25 monomer units are obtained in high yields with a purity that is sufficient for most molecular biological applications, the portion of failure sequences contaminating the target product increases rapidly with longer sequences. Hence, purification and quality control are obligatory, particularly for longer synthetic DNA sequences [35]. In fact, the chromatographic analysis of the raw product of an 80-mer synthesis revealed a number of impurities in the target sequence (Fig. 6). The peaks eluting before

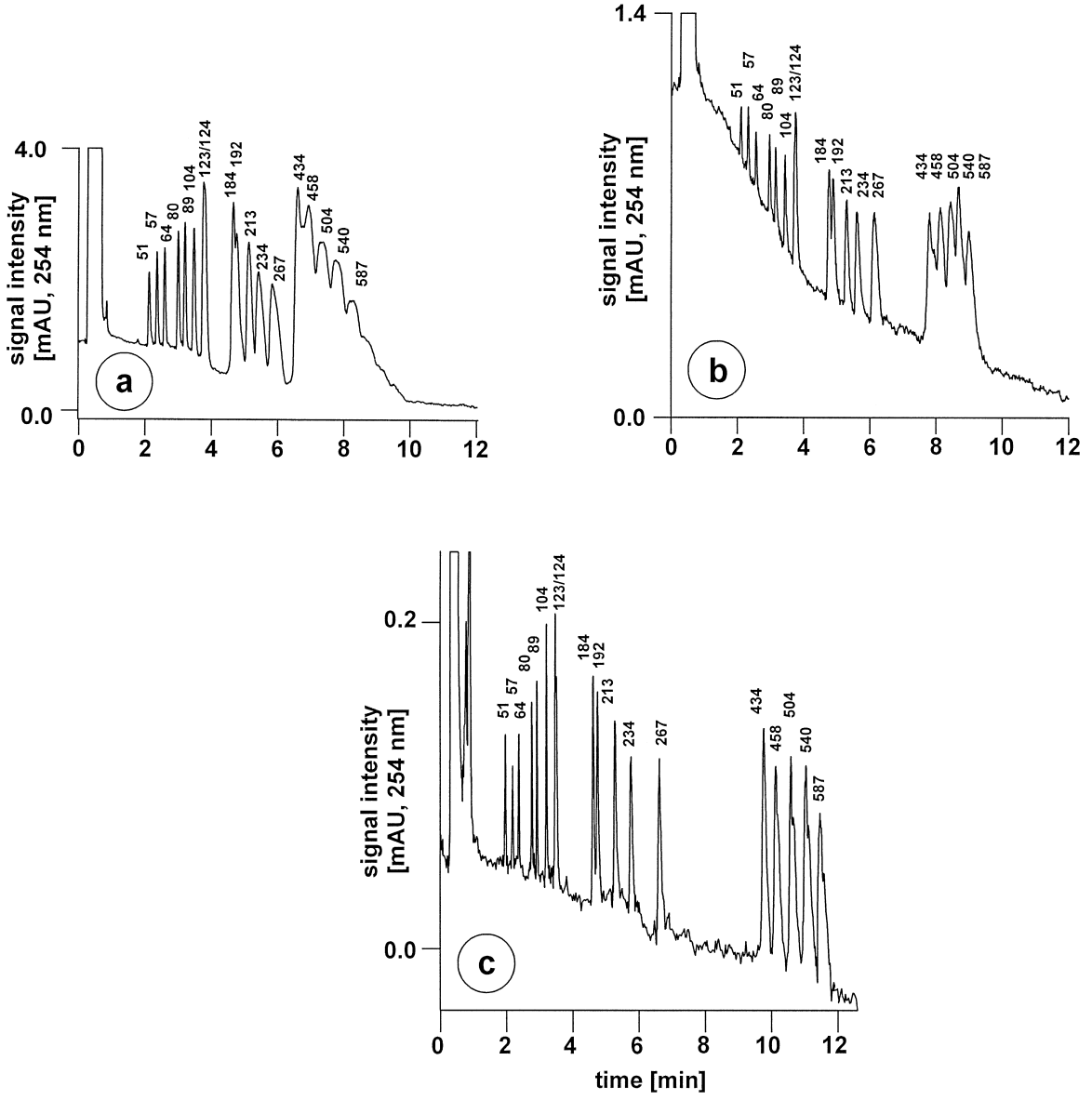

Fig. 5. Analysis of DNA fragments from a pBR322 DNA-*Hae* III digest by capillary IP-RP-HPLC. Column, PS–DVB–C_{18}, 2.1 μm, 60×0.20 mm I.D. with silica frit; mobile phase, (A) 100 m*M* TEAA, pH 7.0, (B) 100 m*M* TEAA, pH 7.0, 20% acetonitrile; linear gradient, 35–67% B in 3.0 min, 67–87% B in 12.0 min; flow-rate, 2.5 μl/min; detector/detection cell, No. 3 in (a) and (b), 4 in (c); sample, (a) 490 ng, (b) 49 ng, (c) 4.6 ng pBR322 DNA-*Hae* III digest.

the target product are usually failure sequences due to incomplete coupling cycles during solid-phase synthesis. IP-RP-HPLC on-line coupled with electrospray mass spectrometry (ESI-MS), readily identified the peak eluting at 7.9 min as the 80-mer target sequence [36]. Moreover, we were recently able to demonstrate that impurities eluting after the target product are target sequences bearing various numbers of protecting groups as a consequence of incomplete deprotection after solid-phase synthesis [27]. The identification of failure sequences in the highly complex reaction mixture of the synthetic

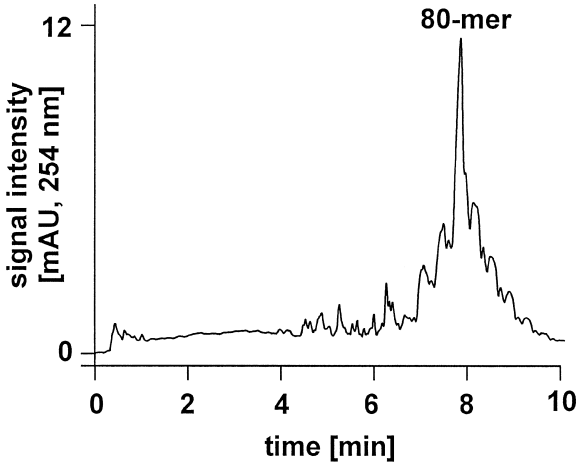

Fig. 6. Purity control of a synthetic 80-mer oligonucleotide. Column, PS–DVB–C_{18}, 2.1 μm, 70×0.20 mm I.D. with silica frit; mobile phase, (A) 100 m*M* TEAA, pH 7.0, (B) 100 m*M* TEAA, pH 7.0, 20% acetonitrile; linear gradient, 0–100% B in 10.0 min; flow-rate, 3.3 μl/min; detector/detection cell, No. 3; sample, synthetic 80-mer raw product, 24.6 ng.

80-mer by IP-RP-HPLC–ESI-MS was difficult, because different failure sequences seem to coelute in the various peaks before the main peak making the interpretation of the resulting mass spectra practically impossible. Nevertheless, this kind of rapid analysis of very small amounts of synthetic oligonucleotides by capillary IP-RP-HPLC is eminently suitable to control the effectiveness of a given chemical synthesis and to estimate the synthesis yield on the basis of peak areas.

3.5. Application of capillary IP-RP-HPLC to the separation of DNA restriction fragments

Separation and fractionation of DNA restriction fragments is a key element in various molecular biological experiments, including cloning, DNA sequencing, genome fingerprinting, and DNA hybridization. The mixture of fragments generated by the enzymatic cleavage of DNA with restriction endonucleases may range from a few base pairs to thousands of base pairs, depending on DNA size, DNA sequence and the restriction enzyme used. Fig. 7a shows the separation of a mixture of DNA fragments ranging in size from 51 to 622 bp by capillary IP-RP-HPLC applying a gradient of 9.25–

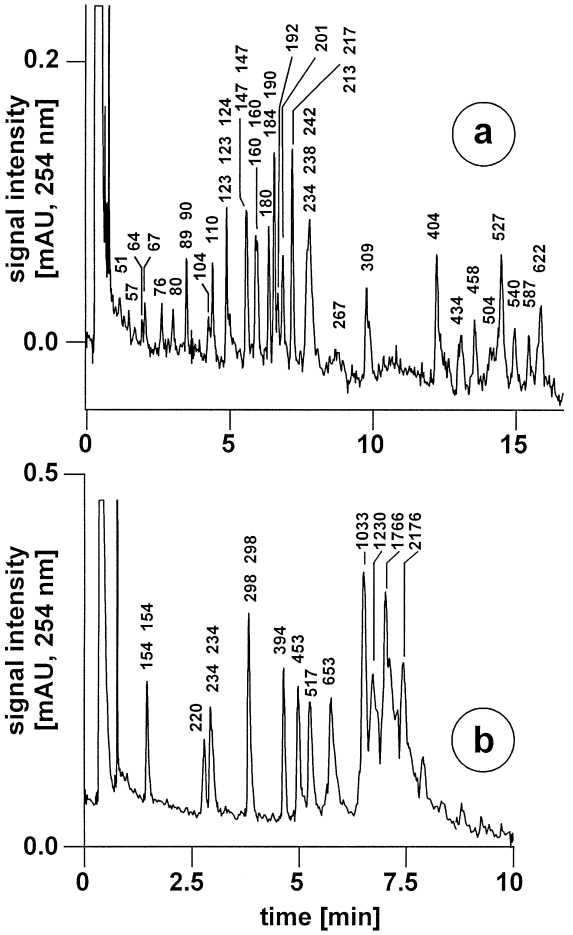

Fig. 7. Capillary IP-RP-HPLC separation of DNA fragments ranging in size from 51 to 2176 base pairs. Column, PS–DVB–C_{18}, 2.1 μm, 60×0.20 mm I.D. with silica frit; mobile phase, (A) 100 m*M* TEAA, pH 7.0, (B) 100 m*M* TEAA, pH 7.0, 25% acetonitrile; linear gradient, (a) 37–55% B in 6.0 min, 55–63% B in 14.0 min, (b) 50–63% B in 5.0 min, 63–68% B in 5.0 min; flow-rate, 2.0 μl/min; detector/detection cell, No. 4; sample, (a) 3.8 ng pBR322 DNA-*Hae* III and 3.8 ng pBR322 DNA-*Msp* I digest, (b) 2.5 ng pBR328 DNA-*Bgl* I and 2.5 ng pBR328 DNA-*Hinf* I digest.

13.75% acetonitrile in 6.0 min, followed by 13.75–15.75% in 14.0 min in 100 m*M* triethylammonium acetate at a flow-rate of 2.0 μl/min. From the 37 fragments detected in the chromatogram, 34 fragments are of different length and could be resolved at least partially into 29 peaks. The total amount of DNA separated in this chromatogram was 7.6 ng, corresponding to approximately 1.4 fmol for each

DNA fragment. This demonstrates the low mass detection limits attainable with capillary IP-RP-HPLC. Moreover, focusing of the biopolymers at the top of the chromatographic bed at low solvent strength during gradient elution allows the injection of relatively large sample volumes without loss of separation efficiency. Therefore, as demonstrated in Fig. 7a, concentration detection limits in the low nanomol per liter range are possible through the injection of low femtomol amounts of DNA fragments in an injection volume of 500 nl. Fig. 7b depicts another example for the separation of DNA restriction fragments by capillary IP-RP-HPLC. The mixture of a *Bgl* I and *Hinf* I digest of the pBR328 plasmid is composed of 15 fragments covering a size range from 154 to 2176 bp. 5.0 ng of this mixture were injected onto the capillary column and eluted with a gradient of 12.5–15.75% acetonitrile in 5 min, followed by 15.75–17.0% in 5 min.

3.6. Application of capillary IP-RP-HPLC to the analysis of PCR products

Today, PCR is one of the most important and widespread tools in biochemistry, molecular biology, and clinical diagnostics [37]. The PCR has also strongly enhanced the usefulness of forensic DNA profiling techniques, as it allows the targeted in vitro amplification of short segments of genomic DNA [38]. Additionally, PCR-based DNA typing systems have made it possible to analyze minute amounts of DNA obtained from only a few cells as well as from highly degraded human remains. With the introduction of short tandem repeat (STR) loci that are amplified by PCR, reliable and simple systems became available for forensic stain typing. Following the PCR process, the amplified DNA fragments have to be separated from the other reaction components, including DNA polymerase, oligonucleotide primers, mononucleotides, and buffer components before their identification and quantitation. Fig. 8 shows the chromatographic analysis of PCR products related to two different alleles of the human tyrosine hydroxylase locus, namely allele 9.3 yielding an 82 bp PCR product, and allele 10 yielding an 83 bp PCR product. In order to resolve the different species present in the PCR mixture, a rather shallow gradient of 7.0–20% acetonitrile in 10 min was used for this separation, although steeper gradients are applicable to speed up the separation. This example demonstrates that capillary IP-RP-HPLC is highly suited to analyze PCR products within a few min. The advantages of IP-RP-HPLC over traditional slab gel or capillary gel electrophoretic methods for the analysis of PCR products are that samples can be analyzed without any prior sample preparation, that the result can be obtained in a short period of time, and that hundreds of samples can be analyzed automatically [39]. However, to make capillary IP-RP-HPLC useful for forensic typing, identification of fragment size by mass spectrometry is necessary.

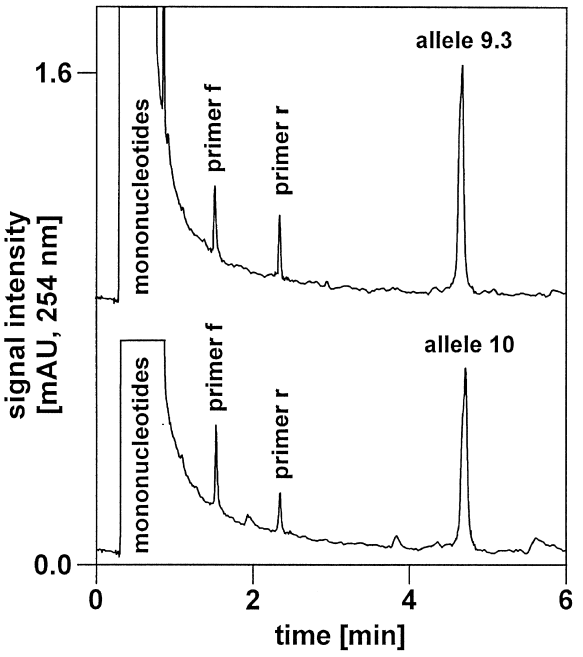

Fig. 8. Analysis of polymerase chain reaction products related to the human tyrosine hydroxylase STR locus. Column, PS–DVB–C_{18}, 2.1 μm, 60×0.20 mm I.D. with PS–DVB frit; mobile phase, (A) 100 m*M* TEAA, pH 7.0, (B) 100 m*M* TEAA, pH 7.0, 20% acetonitrile; linear gradient, 35–100% B in 10.0 min; flow-rate, 2.0 μl/min; detector/detection cell, No. 4.

4. Conclusions

It has been demonstrated, that oligonucleotides and double stranded DNA fragments can be separated in 200 μm I.D. capillary columns packed with

micropellicular, octadecylated PS–DVB particles with a separation efficiency which is equivalent to that obtained with analytical 4.6 mm I.D. columns. Proper design of capillary HPLC instrumentation, especially the miniaturization of connecting and detection volumes, as well as the development of appropriate techniques for preparing frits and packing efficient capillary columns still remain the most critical steps determining the successful application of capillary HPLC to nucleic acid separations. With detection limits in the low femtomol range, capillary IP-RP-HPLC with UV absorbance detection can be applied to the routine analysis of nucleic acids in real samples such as synthetic oligonucleotides, DNA restriction fragments, and PCR products.

Acknowledgements

This work was supported by a grant from the Austrian Science Fund (P13442). The help of J.-P. Chervet from LC packings, Amsterdam, Netherlands, with the optimization of the detector/detection cell configurations is gratefully acknowledged. The authors would like to thank R. Mühlmann (Institute of Legal Medicine) for technical assistance.

References

[1] M.D. Luque de Castro, C. Gamiz-Gracia, Anal. Chim. Acta 351 (1997) 23.
[2] B. He, N. Tait, F.E. Regnier, Anal. Chem. 70 (1998) 3790.
[3] J.E. Battersby, A.W. Guzzetta, W.S. Hancock, J. Chromatogr. B 662 (1994) 335.
[4] M. Novotny, J. Chromatogr. B 689 (1997) 55.
[5] K.-E. Karlsson, M. Novotny, Anal. Chem. 60 (1988) 1662.
[6] R.T. Kennedy, J.W. Jorgenson, Anal. Chem. 61 (1989) 1128.
[7] W.M.A. Niessen, J. van der Greef, Liquid Chromatography–mass Spectrometry: Principles and Applications, Marcel Dekker, New York, 1992.
[8] A.L. Yergey, C.G. Edmonds, I.A.S. Lewis, M.L. Vestal, Liquid Chromatography/mass Spectrometry — techniques and Applications, Plenum Press, New York, 1990.
[9] G. Crescentini, F. Bruner, F. Mangani, G. Yafeng, Anal. Chem. 60 (1988) 1659.
[10] J. Hirata, J. Microcol. Sep. 2 (1990) 214.
[11] J.P.C. Vissers, H.A. Claessens, J. Laven, C.A. Cramers, Anal. Chem. 67 (1995) 2103.
[12] S. Hsieh, J.W. Jorgenson, Anal. Chem. 68 (1996) 1212.
[13] C.G. Huber, P.J. Oefner, G.K. Bonn, Chromatographia 37 (1993) 653.
[14] C.G. Huber, G. Kleindienst, G.K. Bonn, Chromatographia 44 (1997) 438.
[15] C.G. Huber, J. Chromatogr. A 806 (1998) 3.
[16] D.C. Shelly, J.C. Gluckman, M. Novotny, Anal. Chem. 56 (1984) 2990.
[17] J. Gluckman, A. Hirose, V.L. McGuffin, M. Novotny, Chromatographia 17 (1983) 303.
[18] H.J. Cortes, C.D. Pfeiffer, B.E. Richter, T.S. Stevens, J. High-Res. Chromatogr. Chromatogr. Commun. 10 (1987) 446.
[19] R.T. Kennedy, J.W. Jorgenson, Anal. Chem. 61 (1989) 1128.
[20] N.W. Smith, M.B. Evans, Chromatographia 38 (1994) 649.
[21] B. Behnke, J. Johansson, S. Zhang, E. Bayer, S. Nilsson, J. Chromatogr. A 818 (1998) 257.
[22] J.P. Chervet, M. Ursem, J.P. Salzmann, Anal. Chem. 68 (1996) 1507.
[23] K.K. Unger, G. Jilge, U. Esser, H.-J. Schäfer, G. Rathgeber, W. Müller, J. Chromatogr. 476 (1989) 37.
[24] K.-I. Kasai, J. Chromatogr. 618 (1993) 203.
[25] B. Behnke, E. Bayer, J. Chromatogr. A 680 (1994) 93.
[26] J.F. Banks, M. Novotny, J. Chromatogr. 475 (1989) 13.
[27] C.G. Huber, A. Krajete, Anal. Chem. 71 (1999) 3730.
[28] C.G. Huber, P.J. Oefner, G.K. Bonn, Anal. Biochem. 212 (1993) 351.
[29] X. Huang, Cs. Horváth, J. Chromatogr. 788 (1997) 155.
[30] J.P. Chervet, R.E.J. van Soest, An Improved Method of and a Capillary Flow Cell for Analysing Fluid Samples, European Patent Application 0597552A1 (1993).
[31] H. Rebscher, U. Pyell, Chromatographia 38 (1994) 737.
[32] B. Behnke, E. Grom, E. Bayer, J. Chromatogr. A 716 (1995) 207.
[33] C.G. Huber, P.J. Oefner, E. Preuss, G.K. Bonn, Nucl. Acids Res. 21 (1993) 1061.
[34] S.L. Beaucage, M.H. Caruthers, Tetrahedon Lett. 22 (1981) 1859.
[35] C.G. Huber, E. Stimpfl, P.J. Oefner, G.K. Bonn, LC–GC 14 (1996) 114.
[36] A. Premstaller, H. Oberacher, C.G. Huber, Anal. Chem. (2000), in press.
[37] K.B. Mullis, F. Ferre, R.A. Gibbs, The Polymerase Chain Reaction, Springer Verlag, Heidelberg, 1994.
[38] Forensic DNA profiling protocols, P.J. Lincoln, J. Thomson (Eds.), Methods in Molecular Biology, Vol. 98, Humana Press, Totowa, NJ, 1998.
[39] P.J. Oefner, C.G. Huber, E. Puchhammer-Stöckl, F. Umlauft, G.K. Bonn, C. Kunz, BioTechniques 16 (1994) 898.